Direct electrocaloric measurement of $0.9Pb(Mg_{1/3}Nb_{2/3})O_3$-$0.1PbTiO_3$ films using scanning thermal microscopy

S. Crossley[1], T. Usui[2], B. Nair[1], S. Kar-Narayan[1], X. Moya[1], S. Hirose[2], A. Ando[2] and N. D. Mathur[1*]

[1]Materials Science, University of Cambridge, Cambridge, CB3 0FS, UK.
[2]Murata Manufacturing Co. Ltd., Higashikotari 1, Nagaokakyo, Kyoto 617–8555, Japan.
*ndm12@cam.ac.uk

We show that scanning thermal microscopy (SThM) can measure reversible electrocaloric (EC) effects in <40 μm-thick ceramic films of the relaxor ferroelectric $0.9Pb(Mg_{1/3}Nb_{2/3})O_3$-$0.1PbTiO_3$, with the substrate present. We recorded roughly the same non-adiabatic temperature change (±0.23 K) for a thinner film that was driven harder than a thicker film (±31 V μm^{-1} across 13 μm versus ±11 V μm^{-1} across 38 μm), because the thicker film lay relatively closer to the substantially larger adiabatic values that we predicted by thermodynamic analysis of electrical data. Film preparation was compatible with the fabrication of EC multilayer capacitors (MLCs), and therefore our measurement method may be exploited for rapid characterisation of candidate films for cooling applications.

Thermal changes arise when ferroelectric phase transitions are driven by changes of electric field ΔE, but these EC effects are limited to a few kelvin in bulk ceramics[1-4] because $|\Delta E|$ is limited by breakdown to ~10 V μm^{-1}. By contrast, ceramic and polymer films of thickness ≤1 μm show order-of-magnitude larger breakdown fields, resulting in order-of-magnitude larger EC effects (e.g. 12 K with $|\Delta E|$ ~ 100 V μm^{-1})[5,6] that are typically evaluated indirectly[7] from variable-temperature measurements of ferroelectric polarization $P(E)$. Direct measurements of a single film are difficult because small active volumes yield small thermal changes, and these must be both driven and measured on short time scales. Both volume and time-scale problems are exacerbated by the unwanted thermal mass of substrates, which are typically present. Here we use non-contact thermometry to directly measure non-adiabatic temperature change ΔT^* in single ceramic films on substrates. Predictions of adiabatic temperature change ΔT based on the indirect

method confirm that driving and measurement conditions were closer to (further from) the adiabatic limit for our thicker (thinner) film.

Although single EC films could only pump small amounts of heat, many films in multilayer capacitors (MLCs) are attractive for cooling applications[8]. However, the fabrication of bespoke MLCs is slow, so it is preferable to study EC effects in single films fabricated in a manner compatible with MLC fabrication. Direct EC measurements are ultimately desirable, especially because indirect measurements can be unsatisfactory for the following reasons. First, polarization measurements are vulnerable to artefacts[9]. Second, the need for $P(E,T)$ to be single-valued must be reconciled with any thermal or electrical hysteresis, by collecting isothermal data after thermal excursions[10] or by collecting isofield data while varying temperature[7]. Third, any relaxor behaviour should be eliminated by the use of sufficiently high fields. Fourth, adiabatic temperature change ΔT is typically calculated from isothermal entropy change ΔS by assuming that zero-field values of heat capacity may be used to represent finite-field values. That said, it has been shown using magnetocaloric[11,12] and electrocaloric[13] materials that no such assumption is necessary.

Therefore it is exciting to see that EC temperature change has now been directly measured in a small number of films. Free-standing polymer films have been measured using small bead thermistors[14,15]; mass-produced commercial MLCs displaying small serendipitous EC effects have been measured using both resistance thermometry[16] and scanning thermal microscopy (SThM)[17]; both of these sample types have been measured using infra-red thermometry[17,18]; and the optical reflection coefficient of a thin vanadium layer was ingeniously used to make fast measurements of EC temperature change in 150 nm-thick epitaxial films of $Pb(Zr,Ti)O_3$ with substrates present[19]. Direct and indirect EC measurements tend to be equivalent in the absence of non-ergodic relaxor behaviour, but this equivalence can be undermined by concomitant mechanocaloric effects that are invisible to the indirect method[19]. As things stand, agreement between direct and indirect EC measurements has therefore not been hitherto achieved for single ceramic films.

In this paper, we show that SThM can be used to measure EC temperature change in single ceramic films on substrates. SThM is able to detect temperature change in small volumes because it is based on a small thermometer, i.e. the resistance of a Pt track in the tip of an atomic force microscope (AFM). We chose to fabricate our films (and substrates) from $0.9Pb(Mg_{1/3}Nb_{2/3})O_3$-$0.1PbTiO_3$ (PMN-PT), as EC effects of $|\Delta T| \geq 1$ K have recently been reported in $(1-x)Pb(Mg_{1/3}Nb_{2/3})O_3$-$xPbTiO_3$ thin films[20,21], thin bulk platelets[22], free-standing thick films[23], bulk platelets[24], sintered ceramic samples[25] and single crystals[26]. The material is a relaxor, but relaxor

behaviour is not expected at the high fields associated with large EC effects[26-29]. Note that in order to achieve operation near room temperature, our choice of $x = 0.1$ falls below the $x \sim 0.35$ morphotrophic boundary[30] at which EC effects are maximised.

The substrates permitted easy handling and prevented film fracture in the usual way, but they compromised the adiabaticity of our EC temperature-change measurements by acting as thermal anchors. The resulting non-adiabatic values of ΔT^* that we evaluated by room-temperature SThM were therefore smaller than the adiabatic values of ΔT that we subsequently evaluated by the indirect method ($|\Delta T^*| < |\Delta T|$). In principle, this discrepancy could be investigated by modelling experimental heat flow, but it is unlikely that this could be done with sufficient accuracy to eliminate the possible role of any non-ergodic relaxor behaviour.

Two film thicknesses (38 μm and 13 μm) were investigated in order to explore different degrees of departure from adiabaticity (smaller film mass implies faster thermal decay between film and substrate). We did not fabricate thinner films with larger breakdown fields, in view of the following issues. First, a short would be likely to arise from inhomogeneous microstructure if top and bottom electrodes were close enough to be spanned by a single pyrochlore impurity. Second, high breakdown fields can only be achieved in tape-cast films of PMN-PT following grain growth. Third, much thinner films (≤1 μm) would be too thin to measure by SThM. Fourth, slightly thinner films could not be exploited in MLCs, as without structural stability from a substrate there would likely be cracking/delamination both (i) during operation due to non-uniform piezoelectric strain in misaligned grains, and (ii) on cooling to room temperature after processing due to thermal expansion mismatch between films and electrodes. The film thicknesses that we employ here tend to exceed those used in existing MLCs, and could prove relevant for applications.

Sample fabrication was based on the MLC processing method [Fig. 1(a)], and is described with measurement methods in the Supplementary file[31]. Film thicknesses of 13 and 38 μm were established using SEM [Fig. 1(b,c)]. A parasitic pyrochlore phase occupying ~5-10 vol% was revealed using powder X-ray diffraction (XRD). We identified this phase with large grains [bottom of Fig. 1(b), top of Fig. 1(c)] using SEM-EDX (EDX is energy-dispersive X-ray spectroscopy). Dielectric measurements of a 13 μm-thick film at 0.1-100 kHz confirmed the expected[20] presence of a frequency-dependent peak at ~312-324 K [Fig. 2(a)]. The loss tangent [Fig. 2(b)] was an order-of-magnitude larger than the value recorded for sub-micron-thick sol-gel films[20], and comparable with values recorded for sintered ceramic samples[25].

Room-temperature SThM measurements were based on a modification of the well-known[14-18] four-step sequence with two quasi-adiabatic legs and two isofield legs. This modification arose because the quasi-adiabatic legs were rendered non-adiabatic, as the film had intimate contact with the substrate. All four steps were visible for a 38 μm-thick film that was measured using $\Delta E = \pm 10.5$ V μm^{-1} at a tip-sample separation of 20 μm [Fig. 3(a)]. First, field application [$\Delta E > 0$, blue symbols, Fig. 3(a)] generated an EC heat that increased tip temperature [$\Delta T^* > 0$, red symbols, Fig. 3(a)], and EC heat immediately started leaking slowly to the environment. Second, while the applied field was held constant, the continued loss of EC heat eventually restored ambient temperature ($\Delta T^* \sim 0$ at time $t \sim 10$ s). Third, field removal $\Delta E < 0$ produced EC cooling that decreased tip temperature ($\Delta T^* < 0$), and heat immediately started leaking slowly from the environment. Fourth, with no applied field, the continued absorption of heat eventually restored ambient temperature ($\Delta T^* \sim 0$, $t \sim 20$ s). Note that the fast changes in ΔT^* tracked the driving field on its millisecond time scale, prior to a slower change of the same sign. This suggests that heat transfer between tip and sample may be both radiative (fast) and convective (slow). On increasing tip-sample separation to 100 μm [Fig. 3(b)], the fast and slow changes in ΔT^* were both reduced, implying a reduction in both radiative and convective heat transfer.

For each film thickness, the heating ($\Delta T^* > 0$) and cooling ($\Delta T^* < 0$) steps were similar in magnitude, implying negligible Joule heating and good reversibility. The equivalence of heating and cooling steps was also seen when varying $|\Delta E|$ at a reduced tip-sample separation of ~9 μm (Fig. 4, raw data in Supplementary Figs 1&2)[31]. The inverse correlation between breakdown field and sample thickness permitted the thinner film to undergo larger changes of field and therefore larger EC effects, but the greater departure from adiabaticity in the thinner film limited the maximum value of $|\Delta T^*| \sim 0.23$ K to the same value as the thicker film. A critical exponent α for $|\Delta T^*| \propto |\Delta E|^{\alpha}$ was not extracted from measurements of ΔT^* because the $|\Delta T^*(\Delta E)|$ data are noisy.

Next, we will compare our values of ΔT^* with values of ΔT evaluated by the indirect method[7]. This method, which is commonly employed for thin films in view of the difficulty of direct measurements, exploits the Maxwell relation $(\partial S/\partial E)_T = (\partial P/\partial T)_E$ to yield:

$$\Delta T(T,E) = -\frac{T}{\rho c(T)} \int_0^E \left(\frac{\partial P}{\partial T} \right)_{E'} \mathrm{d}E' , \qquad (1)$$

where measured density $\rho = 8030$ kg m^{-3}. We assume $P(E,T)$ to be single valued, and we will neglect the field dependence of specific heat capacity c in the absence of a sharp phase transition,

but in contrast with previous work we will take into account the weak temperature dependence of c (Supplementary Fig. 3)[31]. The assumption that $P(E)$ is single-valued is reasonable, as electrical hysteresis in bipolar $P(E)$ measurements may be avoided by driving EC effects with a unipolar voltage, and we used a voltage that is large enough to exceed the relaxor regime. The assumption that $P(T)$ is single-valued is reasonable, as later we will see that thermal hysteresis is negligible (Supplementary Figs 4-6)[31].

Isothermal $P(E)$ data were obtained every ~0.5 K on heating, and we present the first measurement at 260 K, and the last measurement at 420 K [inset, Fig. 5(a,d)]. For a 38 μm-thick film, we used the same nominal field change (10.5 V μm^{-1}) that we employed for SThM (but we were instrumentally limited to reliably achieving 10.0 and not 10.5 V μm^{-1}). For a 13 μm-thick film, the nominal field change was reduced from 30.8 V μm^{-1} to 19.2 V μm^{-1} in order to avoid fatigue during the many measurements required for data dense in temperature (but we were instrumentally limited to reliably achieving 18.8 and not 19.2 V μm^{-1}). For each film thickness, data from upper $P(E)$ branches in $E > 0$ are presented as $P(T)$ data at selected fields, along with cubic spline fits [Fig. 5(a,d)]. Using Equation (1), all 200 of these fits were used to numerically evaluate $\Delta T(\Delta E)$ up to the highest value of $|\Delta E|$ that we reliably achieved at each of the ~330 values of starting temperature T, and the result is plotted as $\Delta T(\Delta E,T)$ [Fig. 5(b,e)]. For the highest value of $|\Delta E|$, the dependence of ΔT on starting temperature T is plotted as $\Delta T(T)$ [Fig. 5(c,f)]. For each film thickness, heating and cooling data both yield critical exponents ($|\Delta T| \propto |\Delta E|^{\alpha}$) of $\alpha \sim 0.6$ at room temperature (Supplementary Fig. 7(a)[31]), and $\alpha \sim 1.0$ at 390 K away from low $|\Delta E|$ (Supplementary Fig. 7(b)[31]).

For the 38 μm-thick film at room temperature, our maximum value of $|\Delta T| \sim 1.3$ K due to $|\Delta E| \sim 10.0$ V μm^{-1} [$|\Delta T|/|\Delta E| \sim 0.13$ K V^{-1} μm] exceeds the value of $|\Delta T^*| \sim 0.23$ K measured directly using a similar change of field $|\Delta E| \sim 10.5$ V μm^{-1} [$|\Delta T^*|/|\Delta E| \sim 0.02$ K V^{-1} μm], such that $|\Delta T|/|\Delta T^*| \sim 6$. For the 13 μm-thick film at room temperature, our maximum value of $|\Delta T| \sim 1.8$ K due to $|\Delta E| \sim 18.8$ V μm^{-1} [$|\Delta T|/|\Delta E| \sim 0.09$ K V^{-1} μm] exceeds the directly measured value of $|\Delta T^*| \sim 0.23$ K using $|\Delta E| \sim 30.8$ V μm^{-1} [$|\Delta T^*|/|\Delta E| \sim 0.007$ K V^{-1} μm]. Therefore $|\Delta T|/|\Delta T^*| \sim 13$ if we crudely assume $|\Delta T| \propto |\Delta E|$, whereas more precisely we have $|\Delta T|/|\Delta T^*| \sim 10$ if we use $\alpha \sim 0.6$ from above. The variation of $|\Delta T|/|\Delta T^*|$ with film thickness is not a consequence of relaxor behaviour, as the high-field heating and cooling data are highly similar[31]. Instead, the thinner film possessed a smaller value of $|\Delta T^*|$ because it lay further from the adiabatic measurement limit than its thicker counterpart.

On increasing temperature, the increase in $\Delta T(T)$ [Fig. 5(c,f)] is consistent with a field-driven increase of transition temperature [Fig. 2(a)], but we found no clear peak in $\Delta T(T)$ up to our maximum measurement temperature of 420 K. Nevertheless, the 38 μm-thick film shows at 390 K a maximum value of $|\Delta T| \sim 2.6$ K due to $|\Delta E| \sim 10.0$ V μm^{-1} [$|\Delta T|/|\Delta E| \sim 0.26$ K V^{-1} μm], while the 13 μm-thick film shows $|\Delta T| \sim 4.2$ K due to $|\Delta E| \sim 18.8$ V μm^{-1} [$|\Delta T|/|\Delta E| \sim 0.23$ K V^{-1} μm]. These 390 K values of $|\Delta T|/|\Delta E|$ are similar to one another, as are the room-temperature values given above.

A sol-gel film of the same composition was reported to show[20] larger values of $|\Delta T|$ because it could withstand larger electric fields without breakdown, on account of being thinner ($|\Delta T| \sim 5$ K due to 89.5 V μm^{-1} across 350 nm at 333 K). However, our tape-cast films show larger values of $|\Delta T|/|\Delta E|$, both at room temperature where $|\Delta T|/|\Delta E| \sim 0.13$ K V^{-1} μm exceeds the sol-gel value of 0.02 K V^{-1} μm by a factor of six, and also at 390 K where our maximum value of $|\Delta T|/|\Delta E| \sim 0.26$ K V^{-1} μm exceeds the highest sol-gel value of 0.06 K V^{-1} μm at 333 K by a factor of four. These higher EC strengths in thick films are encouraging for applications, and may be attributed to the larger grain size [Fig. 1(c)], a likely reduction in strain, and the likelihood of improved stoichiometry.

The strong similarity of EC behaviour that we infer from data obtained on heating and cooling (Supplementary Figs 4-6)[31] is perhaps surprising in a relaxor, but it is possible for several reasons. First, the relaxor behaviour is suppressed when the applied field is high[26-29]. Second, we operated near and above dielectric peak to avoid glassy behaviour[21]. Third, the phase transition is broad. Fourth, and perhaps most importantly of all, our 2 Hz measurement frequency was sufficiently slow.

In summary, we have used room-temperature SThM to perform direct measurements of non-adiabatic temperature change $|\Delta T^*| \sim 0.23$ K in thick tape-cast films of PMN-PT with substrates present. For the thicker (thinner) film, the EC strength $|\Delta T^*|/|\Delta E|$ was four (six) times less than the indirectly evaluated adiabatic value of $|\Delta T|/|\Delta E|$, as adiabaticity in our direct measurements was compromised to a lesser (greater) extent by the relatively large (small) volume of the film with respect to the substrate. The similarity of our isothermal $P(E)$ data obtained on heating [inset, Fig. 5(a,d)] and cooling[31] demonstrates that the indirect method can be valid for relaxors[26-29]. Validity of the indirect method was ensured by measuring $P(E)$ at low frequency (2 Hz), which we note was only possible because there was no significant d.c. leakage current. This measurement frequency is comparable with frequencies used in EC prototype devices[32-34], suggesting that it may be relevant for practical applications. Moreover, our method of fabricating

films may readily be employed to make the MLCs needed for future EC prototypes[33]. Therefore our overall message is that SThM may be used for high throughput measurements of candidate films for cooling applications.

Acknowledgements

B. N. is grateful for support from Gates Cambridge and the Winton Programme for the Physics of Sustainability. X. M. and S.K.-N. are grateful for support from the Royal Society.

References

[1] P. D. Thacher. Electrocaloric Effects in Some Ferroelectric and Antiferroelectric Pb(Zr, Ti)O_3 Compounds. *J. Appl. Phys.* **39**, 1996 (1968).

[2] W. N. Lawless. Specific heat and electrocaloric properties of $KTaO_3$ at low temperatures. *Phys. Rev. B* **16,** 433 (1977).

[3] B. A. Tuttle and D. A. Payne. The effects of microstructure on the electrocaloric properties of Pb(Zr, Sn, Ti)O_3 ceramics. *Ferroelectrics* **37**, 603 (1981).

[4] L. Shebanov and K. Borman. On lead-scandium tantalate solid solutions with high electrocaloric effect . *Ferroelectrics* **127,** 143 (1992).

[5] A. S. Mischenko, Q. Zhang, J. F. Scott, R. W. Whatmore and N. D. Mathur. Giant electrocaloric effect in thin-film $PbZr_{0.95}Ti_{0.05}O_3$. *Science* **311**, 1270 (2006).

[6] B. Neese, B. Chu, S,-G. Lu, Y. Wang, E. Furman and Q. M. Zhang. Large electrocaloric effect in ferroelectric polymers near room temperature. *Science* **321**, 821 (2008).

[7] X. Moya, S. Kar-Narayan and N. D. Mathur. Caloric materials near ferroic phase transitions. *Nature Mater.* **13,** 439 (2014).

[8] S. Kar-Narayan and N. D. Mathur. Predicted cooling powers for multilayer capacitors based on various electrocaloric and electrode materials. *Appl. Phys. Lett.* **95**, 242903 (2009).

[9] J. F. Scott. Ferroelectrics go bananas. *J. Phys.: Condens. Matter* **20,** 021001 (2008).

[10] L. Caron, Z. Q. Ou, T. T. Nguyen, D. T. Cam Thanh, O. Tegus and E. Brück. On the determination of the magnetic entropy change in materials with first-order transitions. *J. Magn. Magn. Mater.* **321,** 3559 (2009).

[11] H. Wada and Y. Tanabe. Giant magnetocaloric effect of $MnAs_{1-x}Sb_x$. *Appl. Phys. Lett.* **79,** 3302 (2001).

[12] V. K. Pecharsky and K. A. Gschneidner Jr. Giant magnetocaloric effect in $Gd_5(Si_2Ge_2)$. *Phys. Rev. Lett.* **78,** 4494 (1997).

[13] S. Crossley. Electrocaloric Materials and Devices. PhD thesis, Univ. Cambridge (2013); www.repository.cam.ac.uk/handle/1810/245063.

[14] S. G. Lu, B. Rožič, Q. M. Zhang, Z. Kutnjak, R. Pirc, M. Lin, X. Li and L. Gorny. Comparison of directly and indirectly measured electrocaloric effect in relaxor ferroelectric polymers. *Appl. Phys. Lett.* **97**, 202901 (2010).

[15] S. G. Lu, B. Rožič, Q. M. Zhang, Z. Kutnja, and B. Neese. Enhanced electrocaloric effect in ferroelectric poly(vinylidene-fluoride-trifluoroethylene) 55/45 mol% copolymer at ferroelectric–paraelectric transition. *Appl. Phys. Lett.* **98**, 122906 (2011).

[16] S. Kar-Narayan and N. D. Mathur. Direct and indirect electrocaloric measurements using

multilayer capacitors. *J. Phys. D: Appl. Phys.* **43,** 032002 (2010).

[17] S. Kar-Narayan, S. Crossley, X. Moya, V. Kovacova, J. Abergel, A. Bontempi, N. Baier, E. Defay and N. D. Mathur. Direct electrocaloric measurements of a multilayer capacitor using scanning thermal microscopy and infra-red imaging. *Appl. Phys. Lett.* **102**, 032903 (2013).

[18] D. Guo, J. Gao, Y.-J. Yu, S. Santhanam, G. K. Fedder, A. J. H. McGaughey and S. C. Yao. Electrocaloric characterization of a poly(vinylidene flouride-triflouroethylene-chloroflouroethylene) terpolymer by infrared imaging. *Appl. Phys. Lett.* **105,** 031906 (2014).

[19] T. Tong, J. Karthik, R. V. K. Mangalam, L. W. Martin and D. G. Cahill. Reduction of the electrocaloric entropy change of ferroelectric $PbZr_{1-x}Ti_xO_3$ epitaxial layers due to an elastocaloric effect. *Phys. Rev. B* **90,** 094116 (2014).

[20] A. S. Mischenko, Q. Zhang, R. W. Whatmore, J. F. Scott and N. D. Mathur. Giant electrocaloric effect in the thin film relaxor ferroelectric 0.9 $PbMg_{1/3}Nb_{2/3}O_3$–0.1 $PbTiO_3$ near room temperature. *Appl. Phys. Lett.* **89,** 242912 (2006).

[21] T. M. Correia, J. S. Young, R. W. Whatmore, J. F. Scott, N. D Mathur and Q. Zhang. Investigation of the electrocaloric effect in a $PbMg_{2/3}Nb_{1/3}O_3$-$PbTiO_3$ relaxor thin film. *Appl. Phys. Lett.* **95,** 182904 (2009).

[22] H. Uršič, B. Rožič, Z. Kutnjak, J. Holc, M. Kosec, private communication.

[23] B. Rožič, H. Uršič, J. Holc, M. Kosec and Z. Kutnjak. Direct Measurements of the Electrocaloric Effect In Substrate-Free PMN-0.35PT Thick Films on a Platinum Layer. *Integr. Ferroelectr.* **140,** 161-165 (2012).

[24] B. Rožič, M. Kosec, H. Uršič, J. Holc, B. Malič, Q. M. Zhang, R. Blinc, R. Pirc and Z. Kutnjak. Influence of the critical point on the electrocaloric response of relaxor ferroelectrics. *J. Appl. Phys.* **110,** 064118 (2011).

[25] J. Hagberg, A. Uusimäki and H. Jantunen. Electrocaloric characteristics in reactive sintered 0.87 $Pb(Mg_{1/3}Nb_{2/3})O_3$-0.13 $PbTiO_3$. *Appl. Phys. Lett.* **92,** 132909 (2008).

[26] G. Sebald, , L. Seveyrat, D. Guyomar, L. Lebrun, B. Guiffard and S. Pruvost. Electrocaloric and pyroelectric properties of 0.75$Pb(Mg_{1/3}Nb_{2/3})O_3$–0.25$PbTiO_3$ single crystals. *J. Appl. Phys.* **100,** 124112 (2006).

[27] G. G. Guzmán-Verri and P. B. Littlewood. Why is the electrocaloric effect so small in ferroelectrics? http://arxiv.org/abs/1411.1326

[28] T. M. Correia, S. Kar-Narayan, J. S. Young, J. F. Scott, N. D. Mathur, R. W. Whatmore and Q. Zhang. PST thin films for electrocaloric coolers. *J. Phys. D: Appl. Phys.* **44,** 165407 (2011).

[29] F. Le Goupil, A. Berenov, A.-K. Axelsson, M. Valant and N. McN. Alford. Direct and indirect

electrocaloric measurements on <001>-$PbMg_{1/3}Nb_{2/3}O_3$-30$PbTiO_3$ single crystals. *J. Appl. Phys.* **111,** 124109 (2012).

[30] T. R. Shrout, Z. P. Chang, N. Kim, and S. Markgraf. Dielectric behavior of single crystals near the (1−x) $Pb(Mg_{1/3}Nb_{2/3})O_3$-(x) PbTiO3 morphotropic phase boundary. *Ferroelectr. Lett.* **12,** 63 (1990).

[31] See supplemental material for sample fabrication, measurement methods, raw and processed SThM data, heat capacity data, indirect EC data obtained on both heating and cooling, and fits for critical exponents.

[32] Yu. Sinyavsky & V. M. Brodyansky. Experimental testing of electrocaloric cooling with transparent ferroelectric ceramic as working body. *Ferroelectrics* **131,** (1992) 321–325.

[33] H. Gu, X. Qian, X. Li, B. Craven, Z. Wenyi, A. Cheng, S. C. Yao and Q. M. Zhang. A chip scale electrocaloric effect based cooling device. *Appl. Phys. Lett.* **102,** (2013) 122904.

[34] U. Plaznik, A. Kitanovski, B. Rožič, B. Malič, H. Uršič, S. Drnovšek, J. Cilenšek, M. Vrabelj, A. Poredoš and Z. Kutnjak. Bulk relaxor ferroelectric ceramics as a working body for an electrocaloric cooling device. *Appl. Phys. Lett.* **106,** 043903 (2015).

Figure captions

Fig. 1. PMN-PT samples. (a) Schematic showing PMN-PT (yellow) as both substrate and film, with four top electrodes. The bottom electrode is side-contacted. SEM images show PMN-PT films of thickness (b) 13 μm and (c) 38 μm separated from PMN-PT substrates by ~3 μm-thick bottom electrodes. Top electrodes were absent.

Fig. 2. Dielectric behaviour of a 13 μm-thick PMN-PT film. (a) Relative permittivity ε and (b) loss tangent tan(δ) measured on decreasing temperature T.

Fig. 3. Raw SThM data for a 38 μm-thick PMN-PT film at room temperature. For a tip-sample separation of (a) 20 μm and (b) 100 μm, we plot the time t dependence of non-adiabatic temperature change ΔT^* (red) arising due to changes of applied field E (blue). Non-adiabatic temperature change ΔT^* in (a,b) is plotted on a single uncalibrated scale. Field change $|\Delta E| = 10.5$ V μm^{-1} corresponds to voltage change $|\Delta V| = 400$ V. Analogue voltage and temperature signals sampled at 10 kHz.

Fig. 4. SThM results for 13 and 38 μm-thick PMN-PT films at room temperature. Values of non-adiabatic temperature change ΔT^* due to a field change ΔE of the same sign are presented as $|\Delta T^*|$ versus $|\Delta E|$. Vertical bars show spread in raw data (Supplementary Figs 1&2)[31], average values linked by straight lines. Tip-sample separation ~ 9 μm. For each film, the maximum field change (10.5 V μm^{-1} across 38 μm, 30.8 V μm^{-1} across 13 μm) corresponds to a voltage change of 400 V. Raw data sampled at 1 kHz.

Fig. 5. Indirect measurement of EC effects. (a) For a 38 μm-thick film of PMN-PT, we show $P(T)$ (black lines are spline fits) for selected values of field change $|\Delta E|$, derived from isothermal measurements of $P(E)$ at 2 Hz on heating (inset shows two such measurements). The resulting adiabatic temperature change $|\Delta T|$, as a function of starting temperature T, due to (b) field change $|\Delta E|$ and (c) the maximum field change as indicated. Panels (d-f) show the corresponding information for the 13 μm-thick film of PMN-PT. For the film of thickness 38 μm (13 μm), a maximum field change of 10.0 V μm^{-1} (18.8 V μm^{-1}) was reliably achieved using a nominal field change of 10.5 V μm^{-1} (19.2 V μm^{-1}), corresponding to a voltage change of 400 V (250 V).

Figure 1

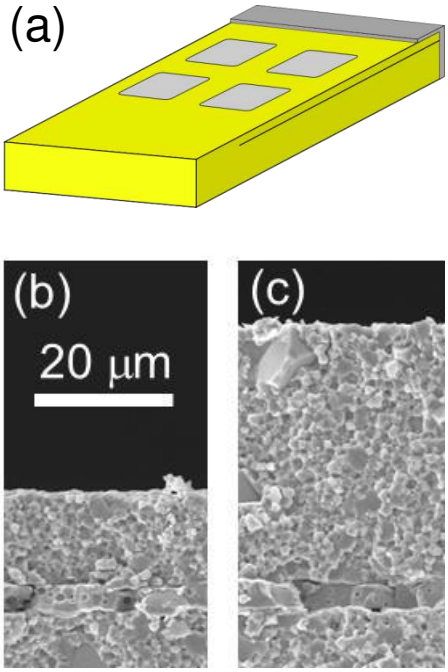

Figure 2

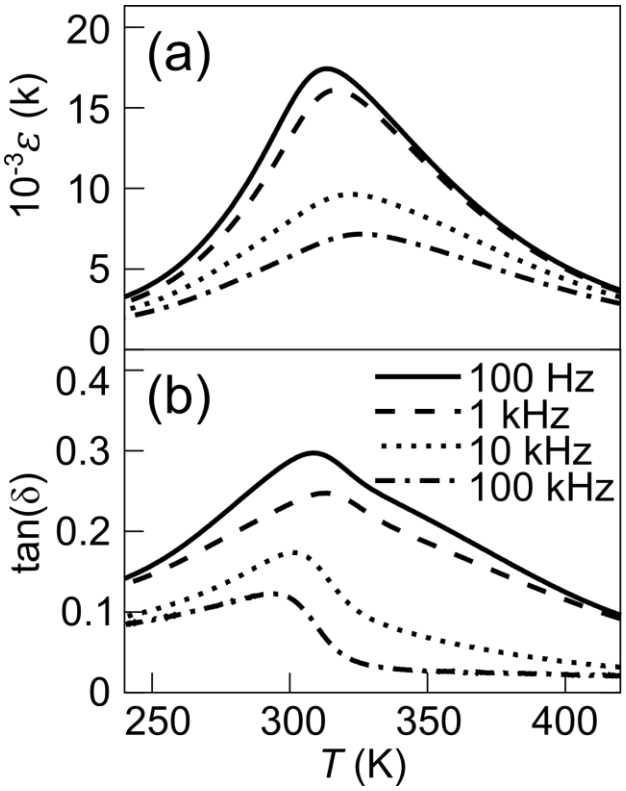
(a)
(b)
$10^{-3}\varepsilon$ (k)
tan(δ)
100 Hz
1 kHz
10 kHz
100 kHz
T (K)
0
5
10
15
20
0.1
0.2
0.3
0.4
250
300
350
400

Figure 3

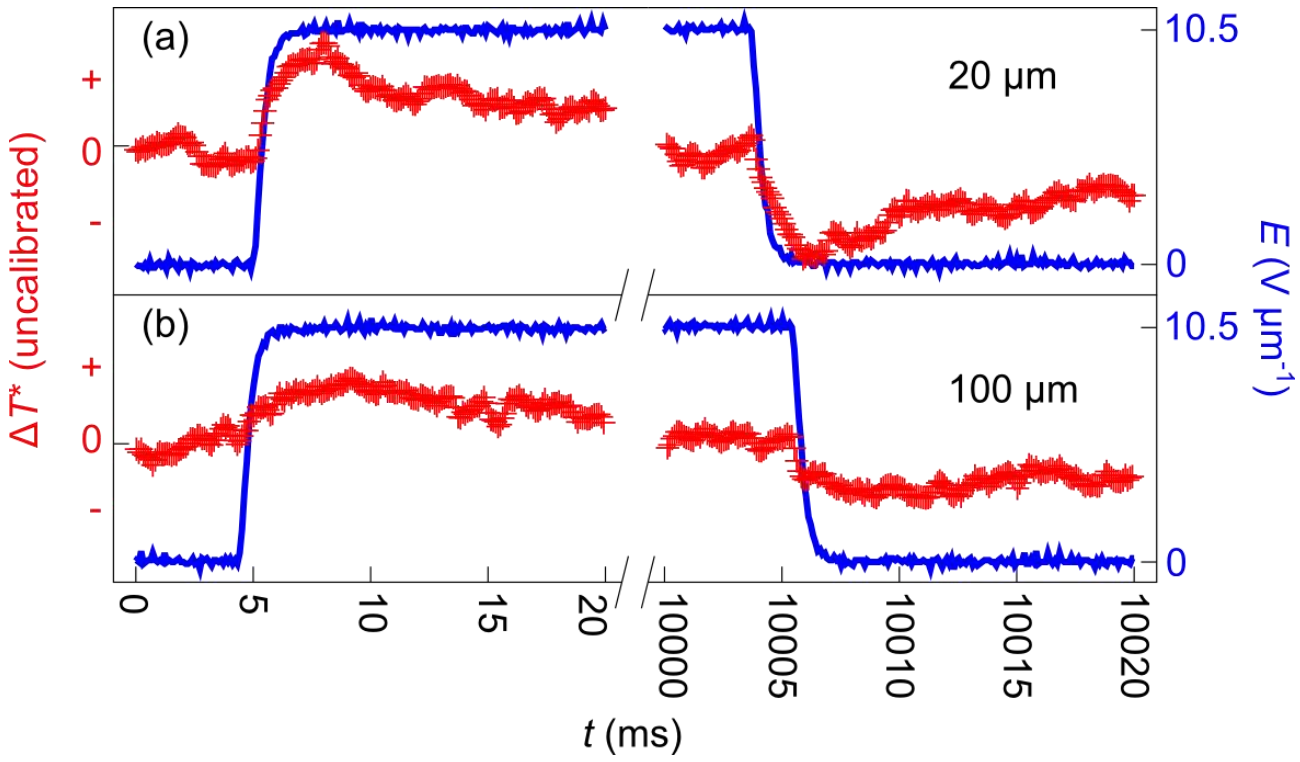
(a)
20 μm
(b)
100 μm
+
0
-
10.5
0
ΔT* (uncalibrated)
E (V μm-1)
0
5
10
15
20
10000
10005
10010
10015
10020
t (ms)

Figure 4

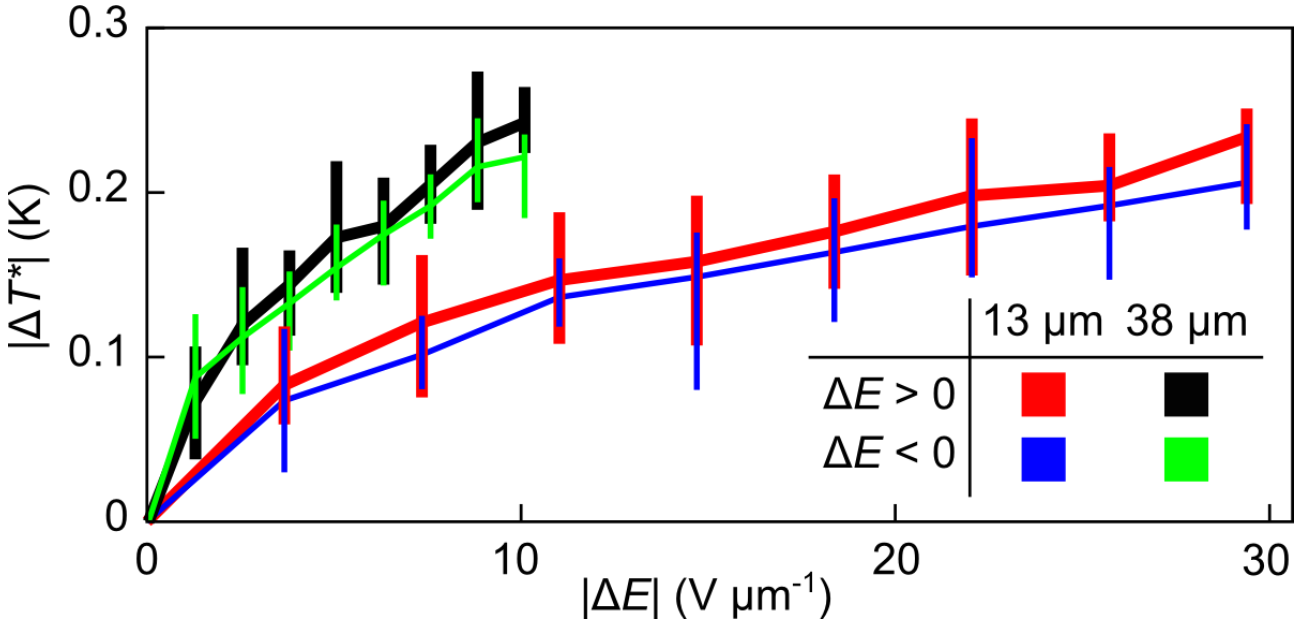

Figure 5

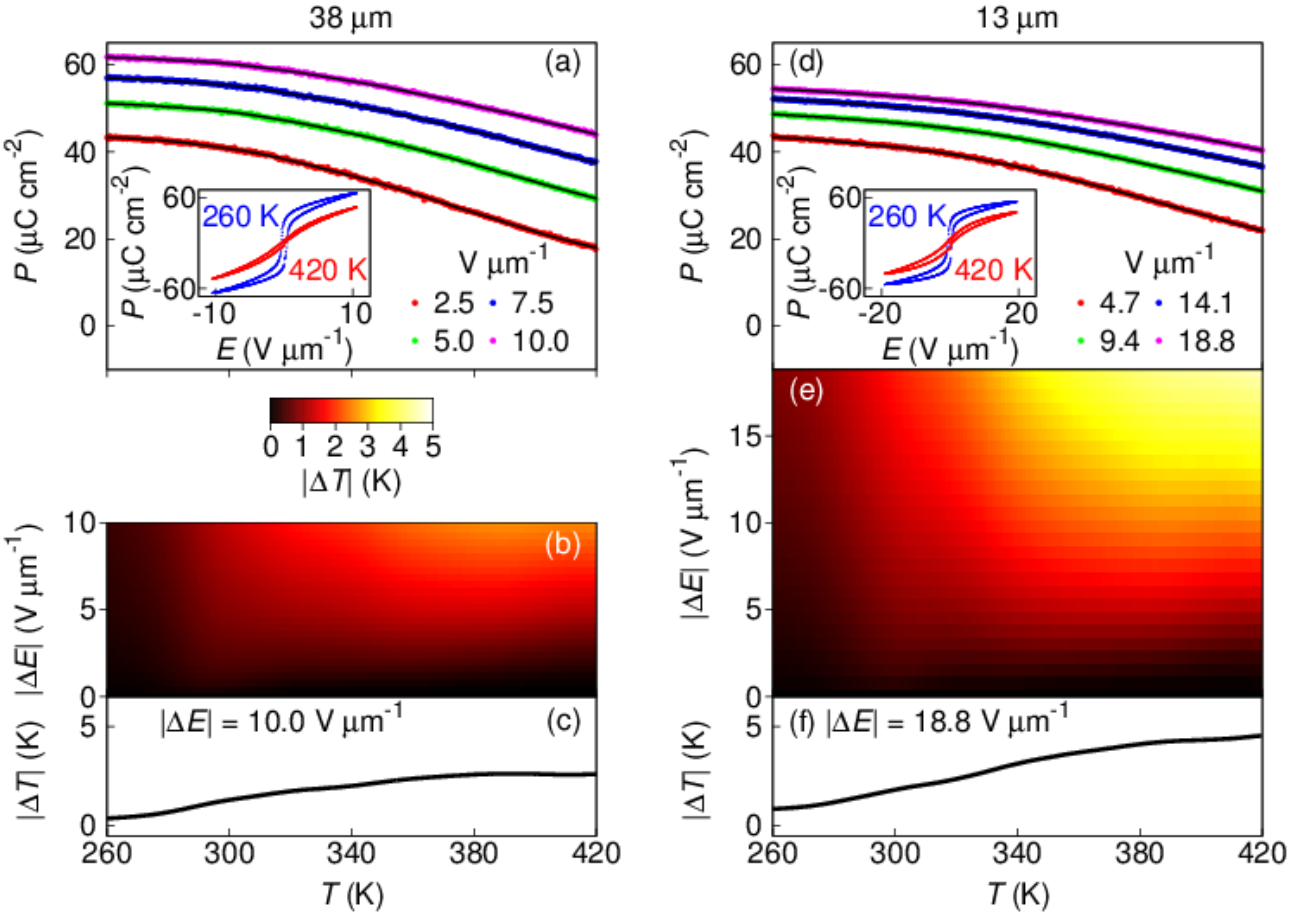
38 μm
13 μm
(a)
(b)
(c)
(d)
(e)
(f)
P (μC cm-2)
E (V μm-1)
260 K
420 K
V μm-1
2.5
5.0
7.5
10.0
4.7
9.4
14.1
18.8
|ΔT| (K)
|ΔE| (V μm-1)
|ΔE| = 10.0 V μm-1
|ΔE| = 18.8 V μm-1
T (K)